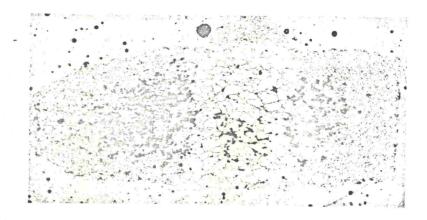
Direct evidence for the gas-containing ability of the particular cell used is shown in Fig. 1 where the ${\rm CrO_2-Cr_2O_3}$ boundary curve becomes essentially coincident with the melting point of the salt liner as a function of pressure at about 1500 °C. The portion of the CrO2 decomposition curve which is dependent on loss of oxygen through the molten salt is in reasonable agreement with the NaCl melting data of Pistorius (15) and checks particularly well with the data of Strong (16) for equipment and cells very similar to that used here. The behavior of the salt liner with respect to gas containment can be observed directly in the form of bubbles in a quenched liner that has been above the melting point. Bubble formation means a rapid loss of oxygen and is accompanied by the rapid formation of $\operatorname{Cr}_2\operatorname{O}_3$. The conversion to $\operatorname{Cr}_2 \operatorname{O}_3$ starts from the outer rim and a partial conversion showing an interface between $\operatorname{Cr}_2 \circ_3$ and Cro_2 is shown in Fig. 2. Conversion to $\operatorname{Cr}_2\operatorname{O}_3$ can also be seen along grain boundaries of the CrO2.



Photomicrograph of cross section of a high-pressure run showing partial conversion of Cr_{02} to Cr_{20_3} after 10 minutes at 1510°C and 50 kb. Bright field. Center part is primarily Cr_{02} with Cr_{20_3} at grain boundaries; Cr_{20_3} predominates on both sides of the center section.